

SUPPORTING INFORMATION

A responsive MOF nanocomposite for decoding volatile organic compounds

You Zhou and Bing Yan*

Shanghai Key Lab of Chemical Assessment and Sustainability, Department of Chemistry, Tongji University, Siping Road 1239, Shanghai 200092, China.

E-mail: byan@tongji.edu.cn.

Experimental

Materials and methods: All chemicals were purchased from commercial sources and used without purification. The ligand 2,2'-bipyridine-5,5'-dicarboxylic acid (H_2bpy) was purchased from Aldrich. $ZrCl_4 \cdot 4H_2O$ was purchased from Adamas. Europium chloride was obtained from europium oxides in HCl (37.5%). Powder X-ray diffraction patterns (PXRD) were recorded with a Bruker D8 diffractometer using $CuK\alpha$ radiation with 40 mA and 40 kV. Nitrogen adsorption/desorption isotherms were measured at liquid nitrogen temperature using a Nova 1000 analyzer. Samples were outgassed for 3 h at 150 °C before measurements. Surface areas were calculated by the Brunauer-Emmett-Teller (BET) method. Thermogravimetric analysis (TG) was measured using a Netzsch STA 449C system at a heating rate of 15 K min⁻¹ under nitrogen protection. Transmission electron microscopy (TEM) was carried out using a JEOL JEM-2100F electron microscope and operated at 200 kV. Inductively coupled plasma-mass spectrometry (ICP-MS) data were collected on an X-7 series inductively coupled plasma-mass spectrometer (Thermo Elemental, Cheshire, UK), the samples were prepared by digesting the dry samples of $Eu^{3+}@bpy-UiO$ into concentrated HNO_3 , followed by the dilution to 0.5% HNO_3 solution. X-ray photoelectron spectroscopy (XPS) experiments were performed on a RBD upgraded PHI-5000C ESCA system (Perkin Elmer) with $MgK\alpha$ radiation ($h\nu = 1253.6$ eV). The photoluminescence spectra and luminescent decay times were examined by an Edinburgh FLS920 phosphorimeter. The absolute external luminescent quantum efficiency was determined employing an integrating sphere (150 mm diameter, $BaSO_4$ coating) from an Edinburgh FLS920 phosphorimeter.

Synthesis of bpy-UiO: The ligand 2,2'-bipyridine-5,5'-dicarboxylic acid (H_2bpydc , 0.248 g, 1 mmol), $ZrCl_4$ (0.233 g, 1 mmol), and glacial acetic acid (2.0 g, 33.33 mmol) were mixed in 60 ml DMF. Glacial acetic acid was added to provide better crystallinity of the product. The mixture was

stirring under ambient conditions for 20 minutes, followed by transferring into a 100 ml Teflon-lined stainless steel container. After heating the Teflon-lined stainless steel container at 393 K for 12 h, a white solid product can be obtained. The resulting white solid was separated from the mixed dispersion by centrifugation and washed with DMF and methanol. To remove the organic species encapsulated within the pores of the open framework, the product was washed with methanol via Soxhlet extraction for 24 h, followed by drying at 333 K under vacuum.

Synthesis of $\text{Eu}^{3+}@\text{bpy}\text{-UiO}$: $\text{Eu}^{3+}@\text{bpy}\text{-UiO}$ was prepared by immersing the bpy-UiO solid in 10 mL methanol solutions of chloride salts of Eu^{3+} (10^{-4} mol) at 333 K for 24 h. The solid was then filtered off and soaked in 15 ml methanol. After 24 h, the supernatant was decanted and replaced by fresh methanol. This procedure was repeated two times to guarantee that the physically adsorbed EuCl_3 salt is removed. Finally, the product was collected by filtration and dried at 333 K under vacuum.

Preparation of $\text{Eu}^{3+}@\text{bpy}\text{-UiO} \supset \text{VOC}$: A methanol activated sample of $\text{Eu}^{3+}@\text{bpy}\text{-UiO}$ (10 mg) was immersed in each liquid (1 mL) at room temperature, resulting in the formation of $\text{Eu}^{3+}@\text{bpy}\text{-UiO} \supset \text{VOC}$.

Figures

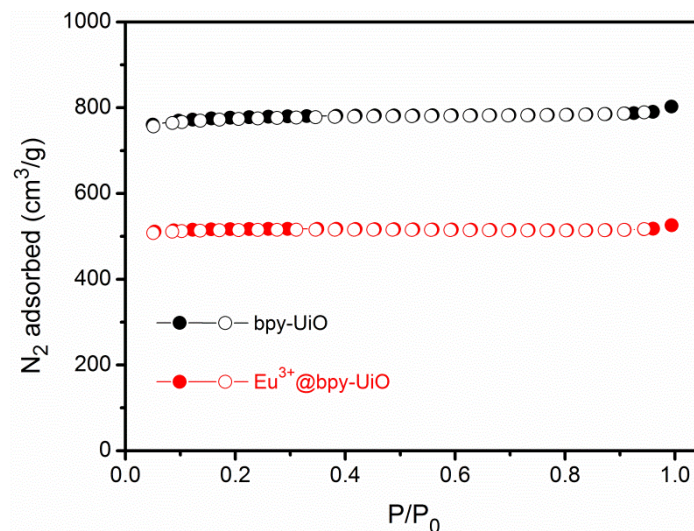


Figure S1. Isotherms for the adsorption of N₂ at 77 K in bpy-UiO (black), Eu³⁺@bpy-UiO (red). Filled and open circles represent adsorption and desorption data, respectively.

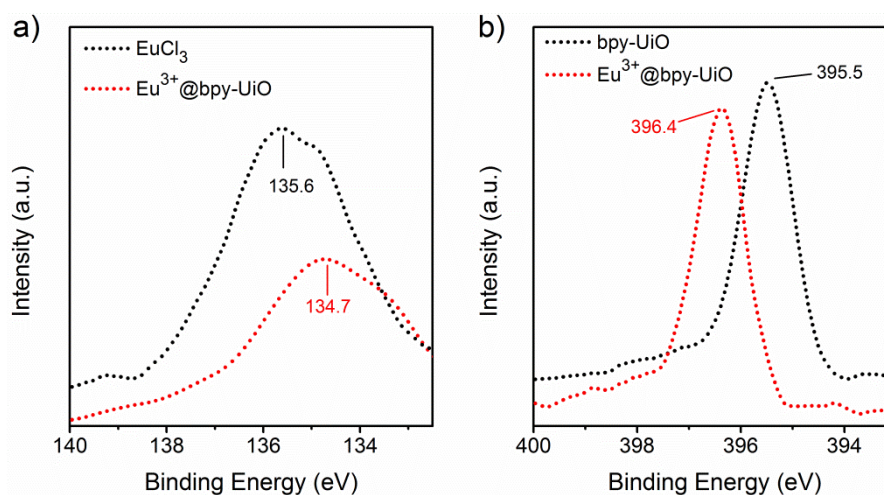


Figure S2. a) Eu4d XPS spectra of EuCl₃ (black) and Eu³⁺@bpy-UiO nanocomposite (red), (b) N1s XPS spectra of bpy-UiO (black) and Eu³⁺@bpy-UiO (red).

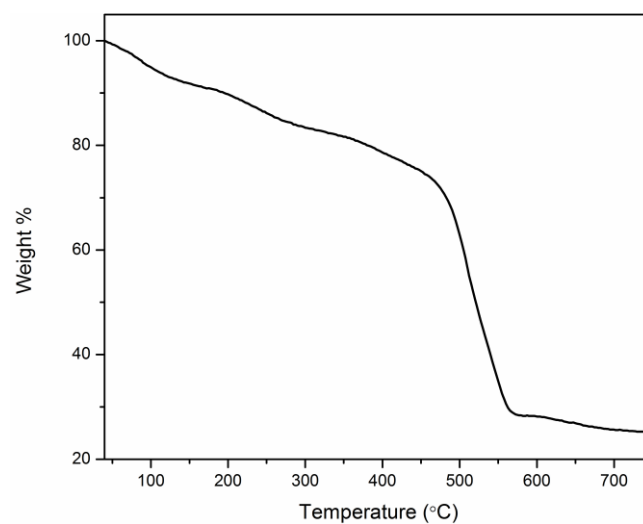


Figure S3. The TG analysis of $\text{Eu}^{3+}@\text{bpy-UiO}$.

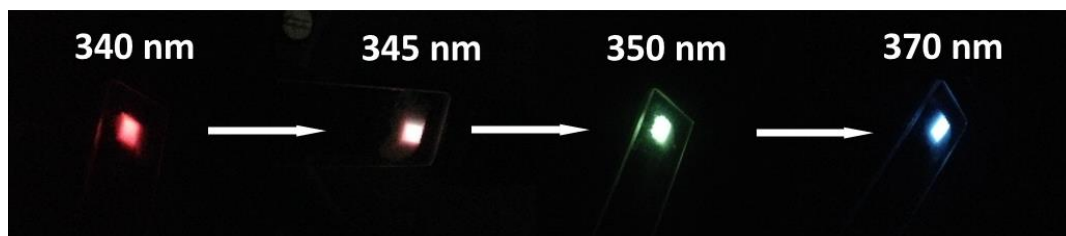


Figure S4. The photographs of $\text{Eu}^{3+}@\text{bpy-UiO}$ upon irradiation at various wavelengths.

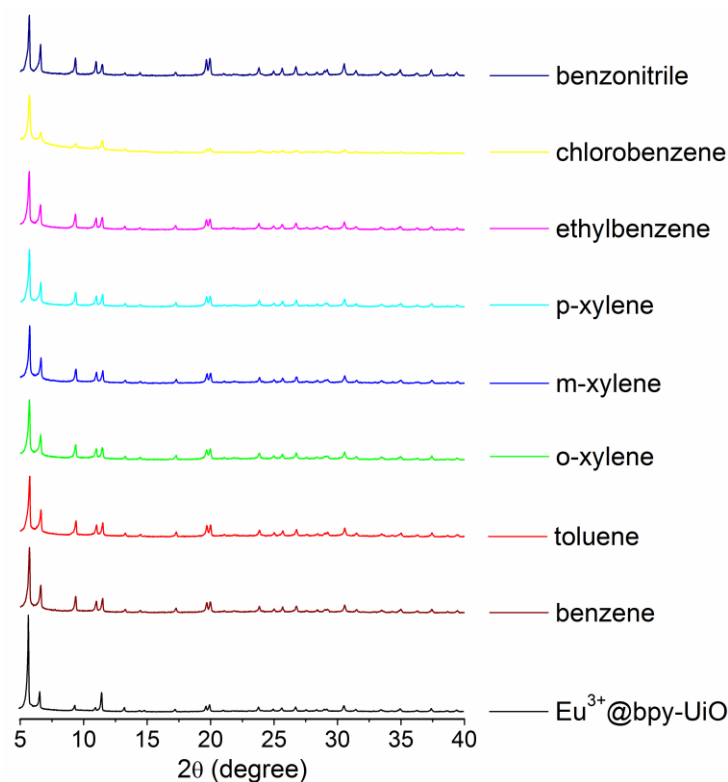


Figure S5. PXRD patterns of different VOCs included Eu^{3+} @bpy-UiO nanocomposite.

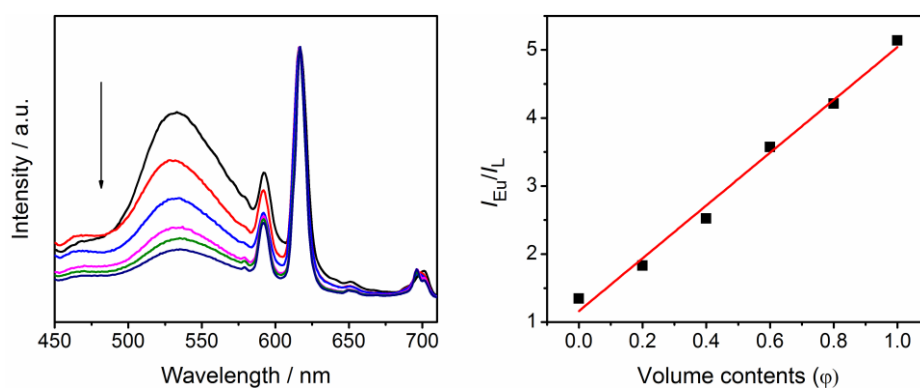


Figure S6. (a) The emission spectra of Eu^{3+} @bpy-UiO suspension in different concentrations of m-xylene cyclohexane solution of 0, 0.2, 0.4, 0.6, 0.8, 1 (volume%, from top to down for ligand emission). The spectra were normalized to the intensity of $^5\text{D}_0 \rightarrow ^7\text{F}_2$ transition of Eu^{3+} . (b) The plot of the intensity ratio of $^5\text{D}_0 \rightarrow ^7\text{F}_2$ transition of Eu^{3+} and bpy ligand emission ($I_{\text{Eu}}/I_{\text{L}}$) as a function of volume contents (ϕ) of m-xylene ranging from 0 to 1. The volume ratio ϕ can be linearly related to $I_{\text{Eu}}/I_{\text{L}}$ with a slope of 3.88.

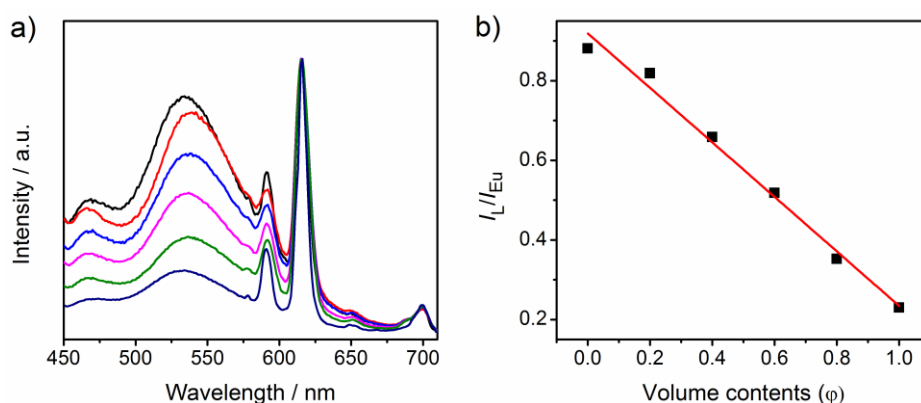


Figure S7. (a) The emission spectra of Eu³⁺@bpy-UiO in methylbenzene, m-xylene, and their mixtures with different volume contents (φ). From top to down for ligand emission: methylbenzene, the mixtures of methylbenzene and m-xylene with m-xylene φ of 0.2, 0.4, 0.6, 0.8, and m-xylene. The spectra were normalized to the intensity of ⁵D₀ → ⁷F₂ transition of Eu³⁺. (b) The plot of the intensity ratio of ⁵D₀ → ⁷F₂ transition of Eu³⁺ and bpy ligand emission (I_L/I_{Eu}) as a function of volume contents (φ) of m-xylene ranging from 0 to 1.

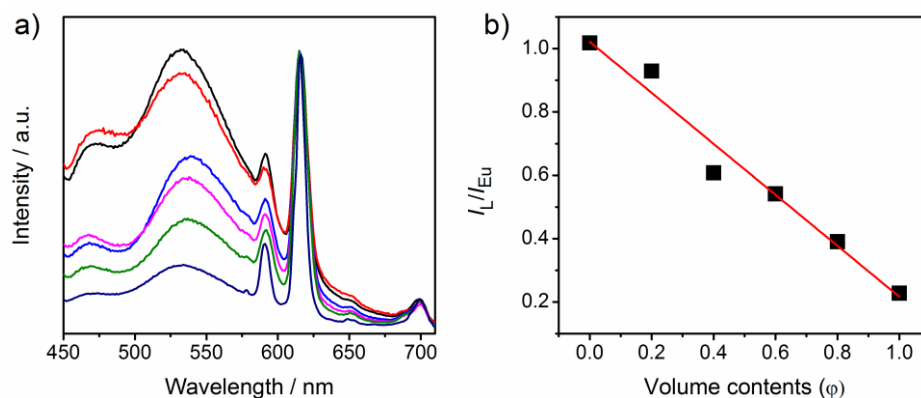


Figure S8. (a) The emission spectra of Eu³⁺@bpy-UiO in ethylbenzene, m-xylene, and their mixtures with different volume contents (φ). From top to down for ligand emission: ethylbenzene, the mixtures of ethylbenzene and m-xylene with m-xylene φ of 0.2, 0.4, 0.6, 0.8, and m-xylene. The spectra were normalized to the intensity of ⁵D₀ → ⁷F₂ transition of Eu³⁺. (b) The plot of the intensity ratio of ⁵D₀ → ⁷F₂ transition of Eu³⁺ and bpy ligand emission (I_L/I_{Eu}) as a function of volume contents (φ) of m-xylene ranging from 0 to 1.

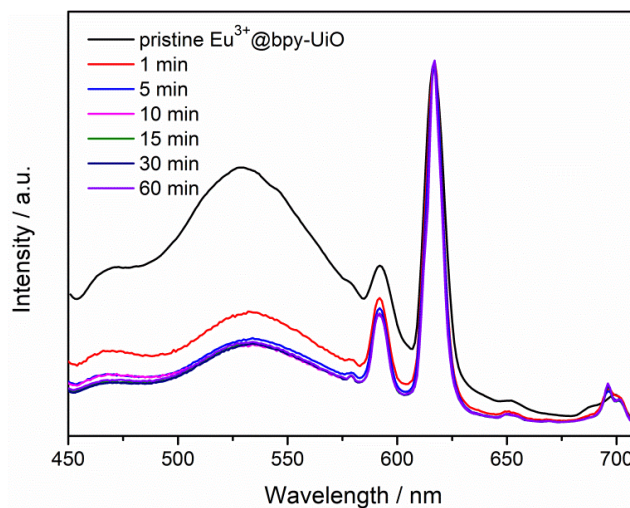


Figure S9. Time-dependent emission spectra of $\text{Eu}^{3+}@\text{bpy-UiO}$ by exposure to m-xylene. The spectra were normalized to the intensity of $^5\text{D}_0 \rightarrow ^7\text{F}_2$ transition of Eu^{3+} .

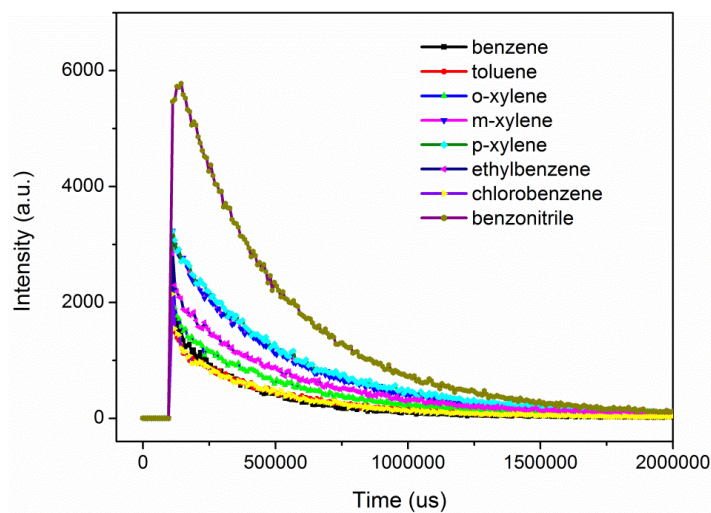


Figure S10. Luminescence decay times ($^5\text{D}_0 \rightarrow ^7\text{F}_2$) of $\text{Eu}^{3+}@\text{bpy-UiO}$ nanocomposite after the adsorption of different VOCs. The excitation wavelength is 355 nm.

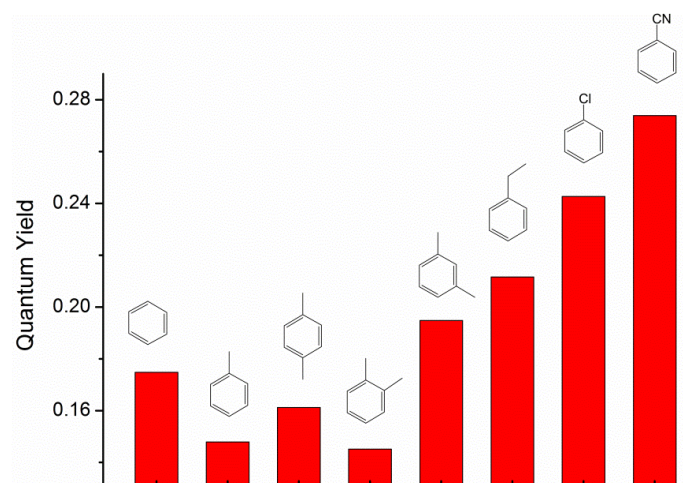


Figure S11. The luminescence quantum yield response of Eu^{3+} @bpy-UiO nanocomposite towards various aromatic VOCs accommodation.

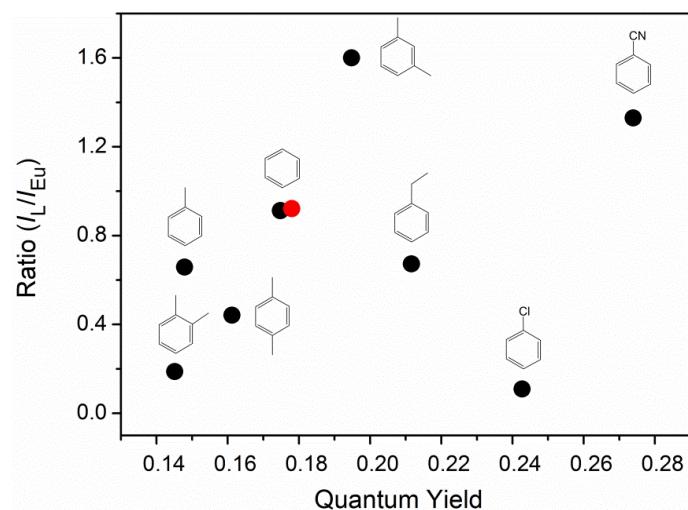


Figure S12. The two-dimensional decoded map demonstrates that the 2D readout (red dot) of an unknown VOC is close to that of benzene, suggesting that the unknown VOC can be recognized as benzene.

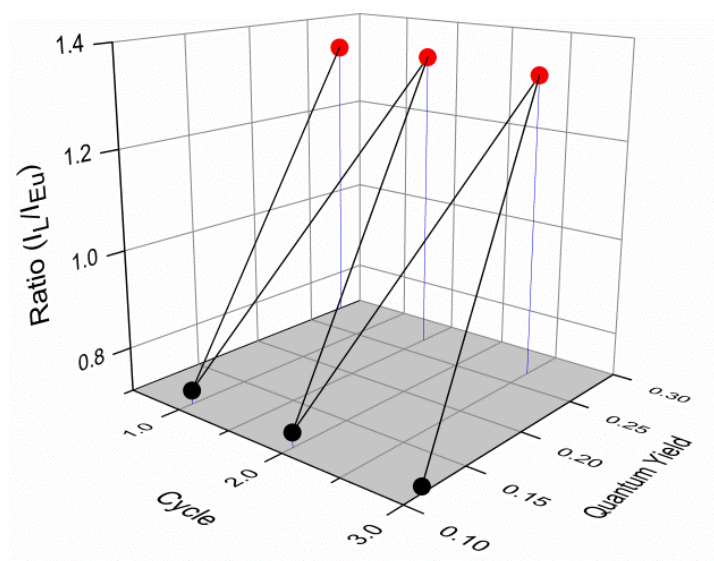










Figure S13. Recycling usage of Eu³⁺@bpy-UiO nanocomposite in sensing benzonitrile molecules for 3 cycles. The red and black dots represent the two-dimensional readouts (I_L/I_{Eu} , ϕ) of the Eu³⁺@bpy-UiO⊃benzonitrile and pristine Eu³⁺@bpy-UiO, respectively.

Table S1. Maximum Eu³⁺ and ligand emission wavelength ($\lambda_{\max-Eu}$, $\lambda_{\max-L}$), and luminescence quantum yields (Φ) of Eu³⁺@bpy-UiO and Eu³⁺@bpy-UiO⊃VOC products.

									
$\lambda_{\max-Eu}$ (nm)	613	613	613	613	613	613	613	613	613
$\lambda_{\max-L}$ (nm)	534	534	538	537	539	527	533	537	532
Φ (%)	11.3	17.5	14.8	16.1	14.5	19.5	21.2	24.3	27.4